Elastomers and Composites
Vol. 50, No. 2, pp. 126~131 (June 2015)

Print ISSN 2092-9676/Online ISSN 2288-7725
DOI: http://dx.doi.org/10.7473/EC.2015.50.2.126

Preparation of C_{60} Nanowhiskers/WO_3 Nanocomposites and Photocatalytic Degradation of Organic Dyes

Keun Hyung Kim*, Jeong Won Ko*, and Weon Bae Ko*,,†**

*Department of Convergence Science, Graduate School, Sahmyook University, Seoul 139-742, South Korea
**Department of Chemistry, Sahmyook University, Seoul 139-742, South Korea

(Received April 29, 2015, Revised May 19, 2015, Accepted May 22, 2015)

Abstract: C_{60} nanowhiskers were synthesized from C_{60} by liquid-liquid interfacial precipitation (LLIP) using C_{60}-saturated toluene and isopropyl alcohol. The WO_3 nanoparticles were synthesized by adding 3.8×10^{-4} mole amount of ammonium metatungstate hydrate ($H_{26}N_6O_{40}W_{12}\cdot H_2O$) to 500 ml of distilled water, and the resulting solution was heated on a hot plate for 4 h. The C_{60} nanowhiskers/WO_3 nanocomposites were prepared with C_{60} nanowhiskers and WO_3 nanoparticles in an electric furnace at 700°C in an argon gas atmosphere for 2 h. The C_{60} nanowhiskers/WO_3 nanocomposites were characterized by X-ray diffraction, scanning electron microscopy, and transmission electron microscopy. UV-vis spectroscopy was used to evaluate the performance of the C_{60} nanowhiskers/WO_3 nanocomposites as a photocatalyst in the degradation of organic dyes, such as methylene blue (MB) and brilliant green (BG) under ultraviolet light (254 nm).

Keywords: C_{60} nanowhiskers, WO_3 nanoparticles, C_{60} nanowhiskers/WO_3 nanocomposites, photocatalyst, degradation of organic dyes

Introduction

The pollution and destruction of the environment all around the world are issues of increasing concern in today's society.[1-4] There is a need for an effective method to remove pollutants.[5-9] Photocatalysis has been widely used as a novel treatment for destroying organic pollutants. Some researchers have demonstrated the advantages of using modified carbon-based semiconductors as photocatalysts, including their strong absorption of visible light and high photocatalytic activity.[10,11]

A new type of C_{60} that takes the form of needle-like crystals, C_{60} nanowhiskers, was synthesized via liquid-liquid interfacial precipitation (LLIP), where the nanowhiskers nucleate at the interface between a toluene solution saturated with C_{60} and isopropyl alcohol.[12-15] The needle crystal of C_{60} nanowhiskers has hexagonal rod shape and diameters ranging from 0.5 to 100 μm. The synthesized single crystal ferroelectric nanowires (FNWs) were less than 1 μm in diameter and greater than 100 μm in length.[14,16,17]

Metal oxide semiconductor photocatalysts have attracted much attention because of their potential applicability to the treatment of wastewater through the photocatalytic degradation of organic compounds. In previous studies, a range of metal oxide semiconductor materials, such as TiO_2, CdS, ZnS, ZnO, and WO_3, have been used to investigate the photocatalytic reduction of pollutants in water.[18,19]

WO_3 nanoparticles are a versatile material that has attracted considerable interest because of its wide-ranging applications in various fields of technology, including electrochromic devices, photocatalysis, gas sensors, and lithium-ion batteries.[20-23] WO_3 nanoparticles have attracted considerable interest because of their photoactive properties, such as their wide response to the solar spectrum due to the size of their band gap (2.8 eV). WO_3 nanoparticles are recognized as not only an important visible-light-responsive photocatalyst but also an excellent electron storage material.[24-28]

Experimental

1. Chemicals

The organic dyes, methylene blue (MB) and brilliant green (BG), and ammonium metatungstate hydrate were purchased

†Corresponding author E-mail: kowb@syu.ac.kr

from Sigma-Aldrich Co.. Ethanol and tetrahydrofuran (THF) were obtained from Samchun Chemicals Co.. C_{60} was supplied by Tokyo Chemical Industry Co..

2. Instruments

An electric furnace (Ajeon Heating Industry Co.) was used to heat the samples, such as C_{60} nanowhiskers, WO_3 nanoparticles, and C_{60} nanowhiskers/WO_3 nanocomposites. A UV lamp (8 W, 254 nm, 77202 Marne La Valee-Cedex1 France) was used as the ultraviolet light source.

The surface of the C_{60} nanowhiskers/WO_3 nanocomposites was observed by scanning electron microscopy (SEM, JEOL Ltd, JSM-6510) at accelerating voltages of 0.5 to 15 kV. The morphology and particle size of the sample were examined with transmission electron microscopy (TEM, JEM-2010, JEOL Ltd.) at an acceleration voltage of 200 kV. The crystal structures of the C_{60} nanowhiskers, WO_3 nanoparticles, and C_{60} nanowhiskers/WO_3 nanocomposites were examined by X-ray diffraction (XRD, Bruker, D8 Advance) using Cu Kα radiation and a secondary monochromator (V = 40 kV, A = 40 mA, Ni filter). UV-vis spectroscopy (Shimadzu UV-1601PC) was performed to characterize the nanomaterials and assess their photocatalytic activity.

Synthesis

1. Synthesis of C_{60} nanowhiskers

In a typical experiment, the C_{60} nanowhiskers were synthesized using the LLIP method. 5 mg of C_{60} was dissolved in 5 mL of toluene for saturation. Isopropyl alcohol (IPA) was added to the C_{60}-saturated toluene solution to form a liquid-liquid interface between the C_{60} saturated solution and IPA. The resulting mixture was maintained at a low temperature for a few days in a refrigerator to obtain C_{60} nanowhiskers.

2. Synthesis of WO_3 nanoparticles

3.8×10^{-4} mole of ammonium metatungstate hydrate ($H_{26}N_6O_{40}W_{12}\cdot H_2O$) was added to 500 mL of distilled water, and the resulting solution was heated for 4 h on a hot plate. The solid state product was calcined in an electric furnace at 800 K for 2 h to synthesize WO_3 nanoparticles.

3. Synthesis of C_{60} nanowhiskers/WO_3 nanocomposites

In a typical experiment, the C_{60} nanowhiskers/WO_3 nanocomposites were prepared with a mass ratio of 1:1. The mixture was dissolved in 10 mL of THF with constant stirring for 30 min. The resulting solution was poured into a vessel, dried to vaporize the organic solvent for 1 h and heated at 800 K in an electric furnace under an argon gas atmosphere for 2 h to obtain the C_{60} nanowhiskers/WO_3 nanocomposites.

4. Photocatalytic degradation of organic dyes with C_{60} nanowhiskers/WO_3 nanocomposites

The photocatalytic activity of the C_{60} nanowhiskers/WO_3 nanocomposites was examined using solutions of MB and BG. 5 mg of the C_{60} nanowhiskers/WO_3 nanocomposites were dispersed into two 10 mL vials of water containing 0.01 mM of either MB or BG. Each vial was irradiated with ultraviolet light at 254 nm. The degradation of the MB and BG solutions with the C_{60} nanowhiskers/WO_3 nanocomposites as a photocatalyst were observed by UV-vis spectroscopy.

Results and Discussion

Figure 1 shows SEM images of (a) the synthesized C_{60} nanowhiskers, (b) the synthesized WO_3 nanoparticles and (c) the C_{60} nanowhiskers/WO_3 nanocomposites. The C_{60} nanowhiskers showed needle-like rod morphology. The WO_3 nanoparticles showed an irregular hexagonal structure and a rock nanobrick-like morphology. The WO_3 nanoparticles were located above the C_{60} nanowhiskers, which had a needle-like rod morphology in the C_{60} nanowhiskers/WO_3 nanocomposites.

Figure 2 shows TEM images of (a) the synthesized C_{60} nanowhiskers, (b) the synthesized WO_3 nanoparticles and (c) the C_{60} nanowhiskers/WO_3 nanocomposites. The C_{60} nanowhiskers were grown by the LLIP method and had a needle-like rod morphology. The WO_3 nanoparticles showed an irregular, broken, rock-like morphology. The C_{60} nanowhiskers/WO_3 nanocomposites showed an agglomerated state, where the WO_3 nanoparticles were adsorbed on the C_{60} nanowhiskers.

Figure 3 shows the XRD patterns of (a) the synthesized C_{60} nanowhiskers, (b) the synthesized WO_3 nanoparticles and (c) the C_{60} nanowhiskers/WO_3 nanocomposites. The C_{60} nanow-

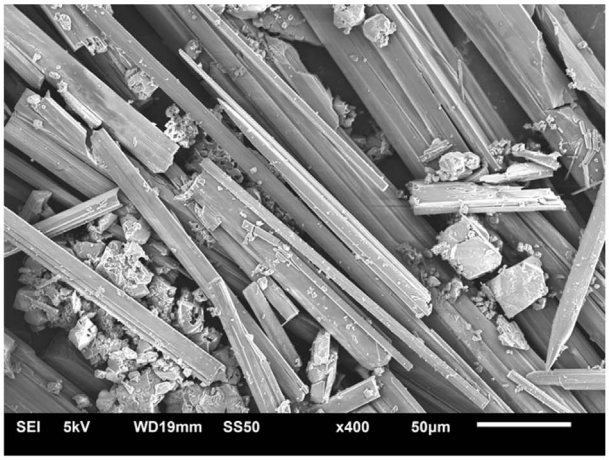

(a)

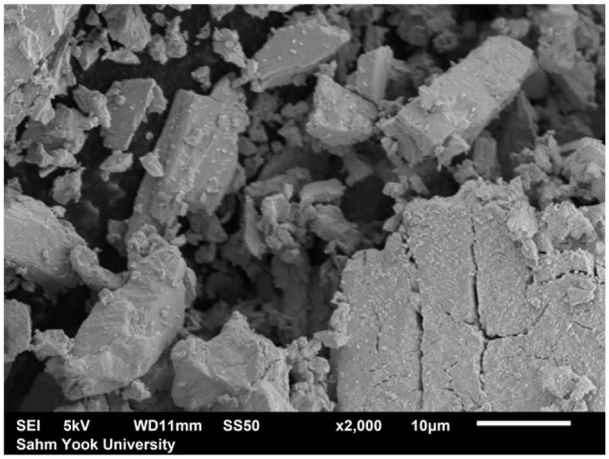

(b)

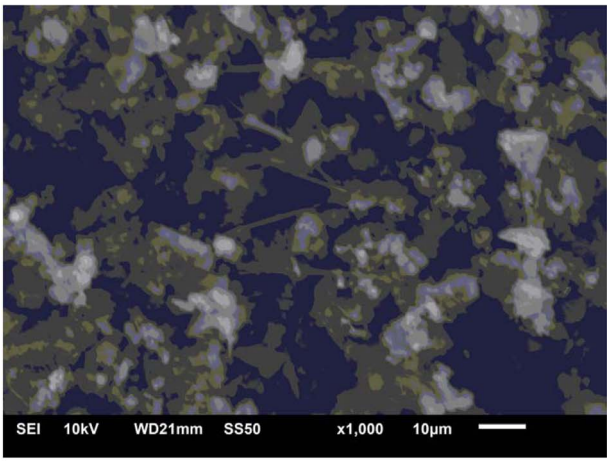

(c)

Figure 1. SEM images of the synthesized (a) C_{60} nanowhiskers, (b) WO_3 nanoparticles, and (c) C_{60} nanowhiskers/WO_3 nanocomposites.

hisker has peaks at 2θ angles of 10.82°, 17.69°, 20.78°, 28.09, 30.49°, and 32.80°, which were assigned to the (111), (220), (311), (420), (422), and (333) planes. The XRD pat-

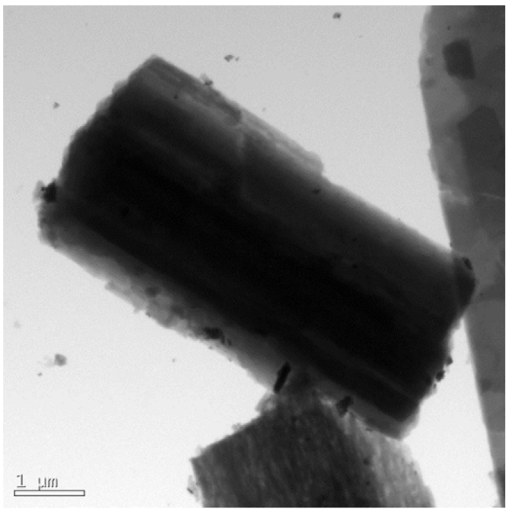

(a)

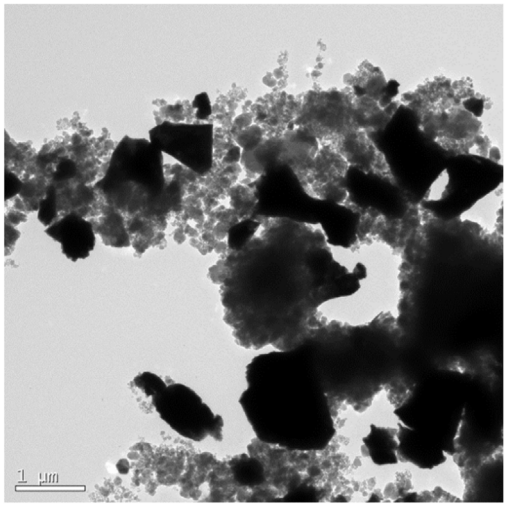

(b)

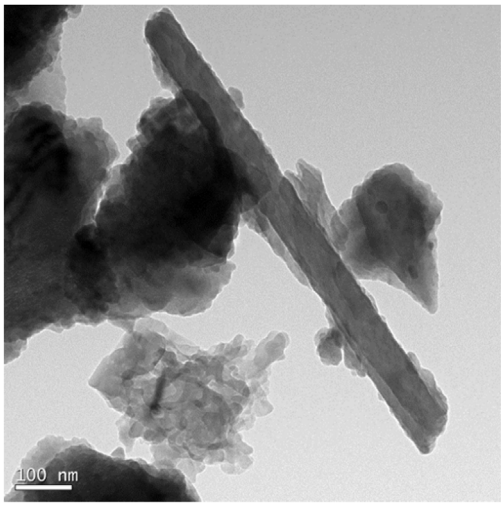

(c)

Figure 2. TEM images of the synthesized (a) C_{60} nanowhiskers, (b) WO_3 nanoparticles, and (c) C_{60} nanowhiskers/WO_3 nanocomposites.

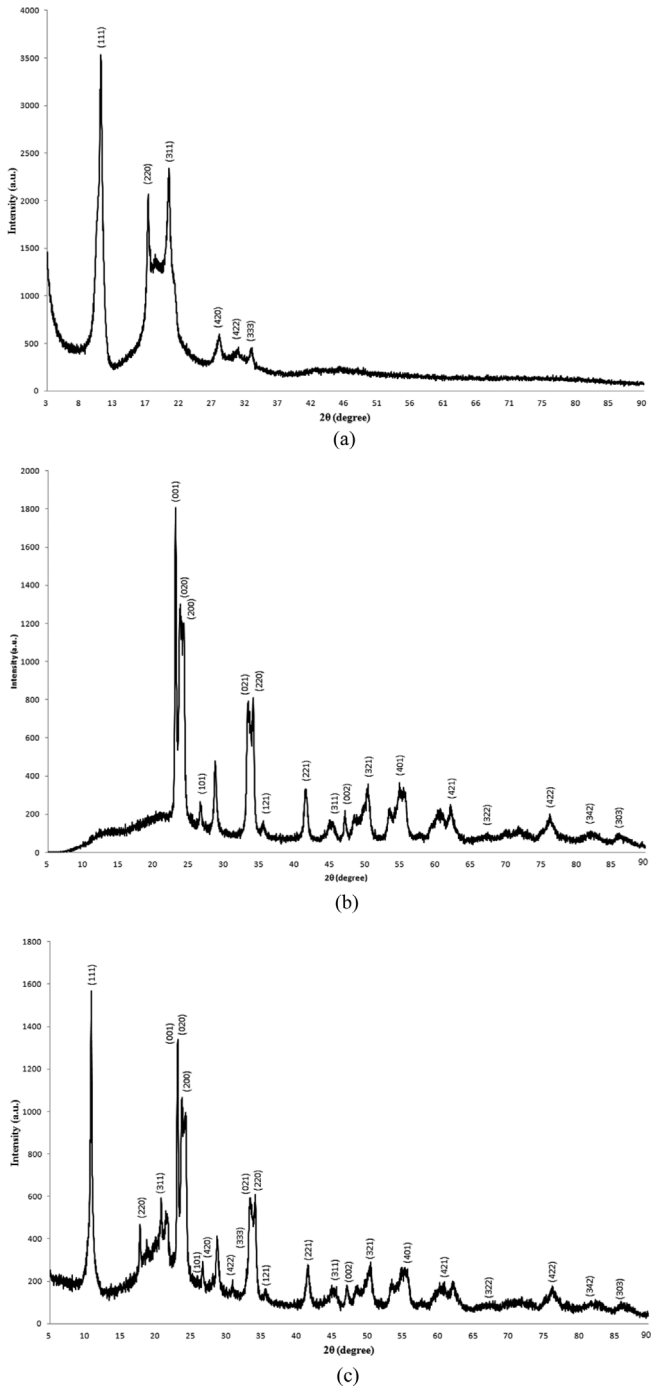

Figure 3. XRD patterns of the synthesized (a) C_{60} nanowhiskers, (b) WO_3 nanoparticles, and (c) C_{60} nanowhiskers/WO_3 nanocomposites.

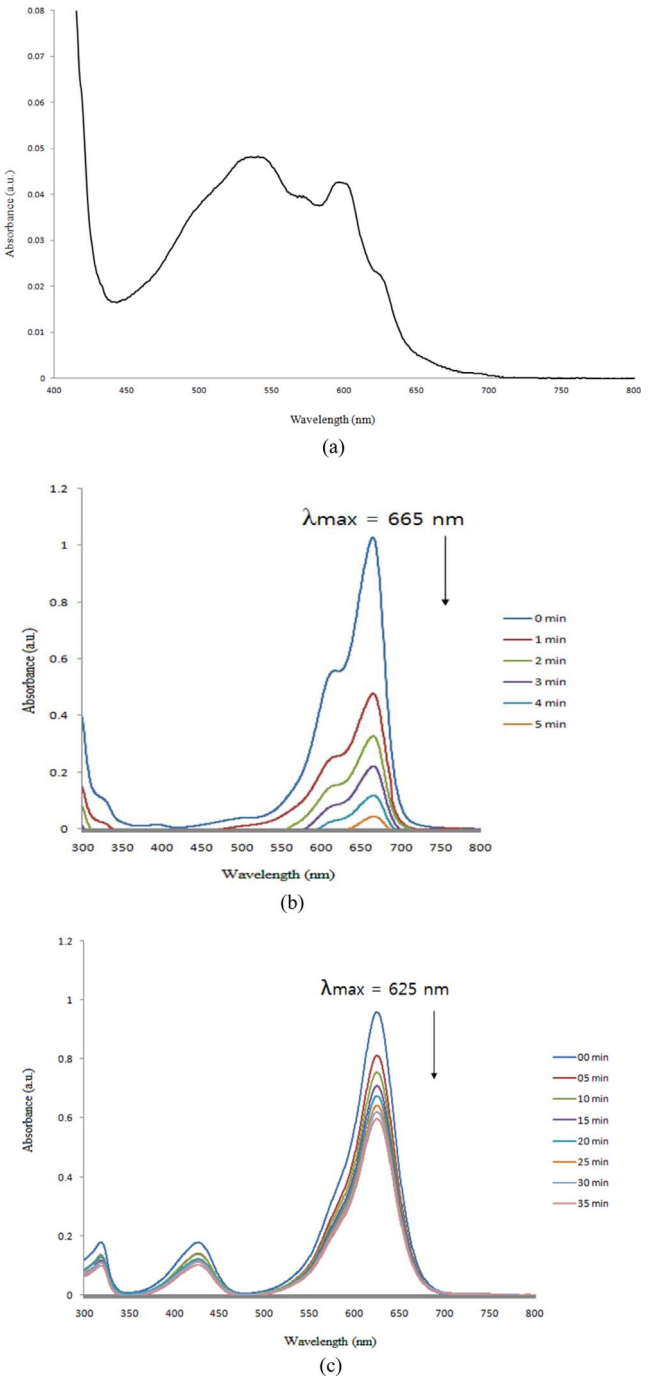

Figure 4. UV-vis spectra of the synthesized (a) C_{60} nanowhiskers, the degradation of (b) methylene blue and (c) brilliant green solution treated with the C_{60} nanowhiskers/WO_3 nanocomposites.

tern of the WO_3 nanoparticles has peaks at 2θ angles of 23.16°, 23.83°, 24.36°, 26.45°, 33.52°, 34.17°, 35.62°, 41.77°, 45.65°, 47.30°, 50.57°, 55.83°, 61.42°, 67.31°, 76.47°, 82.24°, and 86.08°, which were assigned to the (001), (020), (200), (101), (021), (220), (121), (221), (311), (002), (321), (401), (421), (322), (422), (342), and (303) planes. The XRD pattern of the C_{60} nanowhiskers/WO_3 nanocomposites has peaks at 2θ angles of 23.16°, 23.79°, 24.32°, 26.74°, 33.48°, 34.15°, 35.66°, 41.69°, 45.71°, 47.30°, 50.57°, 55.79°, 61.40°, 67.02°, 76.53°, 82.50°, and 86.14° due to the WO_3 nanoparticles, which were assigned to the (001), (020), (200), (101), (021), (220), (121), (221), (311), (002), (321), (401), (421), (322),

(422), (342), and (303) planes, and peaks at 10.87°, 17.70°, 20.81°, 28.04, 30.80°, and 32.81° due to the C_{60} nanowhiskers, which were assigned to the (111), (220), (311), (420), (422), and (333) planes.

Figure 4 shows the UV-vis spectra of (a) the C_{60} nanowhiskers which were synthesized using the LLIP method, the degraded (b) methylene blue (MB) and (c) brilliant green (BG) solution with the C_{60} nanowhiskers/WO_3 nanocomposites under ultraviolet irradiation at 254 nm. The UV-vis spectra of the C_{60} nanowhiskers which were dissolved in toluene revealed peaks at λ_{max} = 542 nm, 597 nm and 622 nm. As a result, MB solution was more effectively degraded than BG solution, comparing the intensity of absorbance of each sample when using the C_{60} nanowhiskers/WO_3 nanocomposites as a photocatalyst.

Conclusion

The C_{60} nanowhiskers had a needle-like rod morphology with a length of 6 μm. The WO_3 nanoparticles had an irregular, broken, rock-like morphology and were less than 2 nm in size. In the C_{60} nanowhiskers/WO_3 nanocomposites, the WO_3 nanoparticles were attached to the sides of the C_{60} nanowhiskers. The length of C_{60} nanowhiskers decreased during calcination, because they might have been broken to a smaller size. The photocatalytic degradation with the C_{60} nanowhiskers/WO_3 nanocomposites was more efficient for MB than BG.

Acknowledgments

This study was supported by Sahmyook University, Korea.

References

1. A. K. Jain, V. K. Gupta, A. Bhatnagar, and Suhas, "A Comparative Study of Adsorbents Prepared from Industrial Wastes for Removal of Dyes", *Sep. Sci. Technol.*, **38**, 463 (2003).
2. V. K. Gupta, I. Ali, and V. K. Saini, "Defluoridation of wastewaters using waste carbon slurry", *Water Res.*, **41**, 3307 (2007).
3. V. K. Gupta, A. Rastogi, and A. Nayak, "Biosorption of nickel onto treated alga (*Oedogonium hatei*): Application of isotherm and kinetic models", *J. Colloid Interface Sci.*, **342**, 533 (2010).
4. A. Mittal, J. Mittal, A. Malviya, D. Kaur, and V. K. Gupta, "Adsorption of hazardous dye crystal violet from wastewater by waste materials", *J. Colloid Interface Sci.*, **343**, 463 (2010).
5. V. K. Gupta, R. Jain, and S. Varshney, "Electrochemical removal of the hazardous dye Reactofix Red 3 BFN from industrial effluents", *J. Colloid Interface Sci.*, **312**, 292 (2007).
6. V. K. Gupta, A. Mittal, A. Malviya, and J. Mittal, "Adsorption of carmoisine A from wastewater using waste materials-Bottom ash and deoiled soya", *J. Colloid Interface Sci.*, **335**, 24 (2009).
7. K. Gupta, R. Jain, and S. Varshney, "Removal of Reactofix golden yellow 3 RFN from aqueous solution using wheat husk-An agricultural waste", *J. Hazard. Mater.*, **142**, 443 (2007).
8. V. K. Gupta, B. Gupta, A. Rastogi, S. Agarwal, and A. Nayak, "A comparative investigation on adsorption performances of mesoporous activated carbon prepared from waste rubber tire and activated carbon for a hazardous azo dye-Acid Blue 113", *J. Hazard. Mater.*, **186**, 891 (2011).
9. V. K. Gupta, A. Mittal, L. Kurup, and J. Mittal, "Adsorption of a hazardous dye erythrosine over hen feathers", *J. Colloid Interface Sci.*, **304**, 52 (2006).
10. Y. Wang, J. Lin, R. Zong, J. He, and Y. Zhu, "Enhanced photoelectric catalytic degradation of methylene blue via TiO_2 nanotube arrays hybridized with graphite-like carbon", *J. Mol. Catal. A Chem.*, **349**, 13 (2011).
11. T. A. Saleh, S. Agarwal, and V. K. Gupta, "Synthesis of MWCNT/MnO_2 and their application for simultaneous oxidation of arsenite and sorption of arsenate", *Appl. Catal. B*, **106**, 46 (2011).
12. K. Miyazawa, Y. Kuwasaki, A. Obayashi, and M. Kuwabara, "C_{60} Nanowhiskers Formed by the Liquid-liquid Interfacial Precipitation Method", *J. Mater. Res.*, **17**, 83 (2002).
13. K. Miyazawa, K. Hamamoto, S. Nagata, and T. Suga, "Structural investigation of the C_{60}/C_{70} whiskers fabricated by forming liquid-liquid interfaces of toluene with dissolved C_{60}/C_{70} and isopropyl alcohol", *J. Mater. Res.*, **18**, 1096 (2003).
14. K. Miyazawa, A. Obayashi, and M. Kuwabara, "C_{60} Nanowhiskers in a Mixture of Lead Zirconate Titanate Sol-C_{60} Toluene Solution", *J. Am. Ceram. Soc.*, **84**, 3037 (2001).
15. K. Miyazawa, Y. Yuwasaki, K. Hamamoto, S. Nagata, A. Obatashi, and M. Kuwabara, "Structural characterization of C_{60} nanowhiskers formed by the liquid/liquid interfacial precipitation method", *Surf. Interface Anal.*, **35**, 117 (2003).
16. Y. Yoshida, "Scanning Electron Microscope Images of C_{60} Whiskers", *Jpn. J. Appl. Phys.*, **31**, L505 (1992).
17. R. M. Fleming, A. R. Kortan, B. Hessen, T. Siegrist, F. A. Thiel, P. Marsh, R. C. Haddon, R. Tycko, G. Dabbagh, M. L.

Kaplan, and A. M. Mujsce, "Pseudotenfold symmetry in pentane-solvated C_{60} and C_{70}", *Phys. Rev. B*, **44**, 888 (1991).
18. S. Bae, E. Shim, J. Yoon, and H. Joo, "Enzymatic hydrogen production by light-sensitized anodized tubular TiO_2 photoanode", *Sol. Energ. Mat. Sol. C*, **92**, 402 (2008).
19. L. Q. Jing, S. D. Li, S. Song, L. P. Xue, and H. G. Fu, "Investigation on the electron transfer between anatase and rutile in nano-sized TiO_2 by means of surface photovoltage technique and its effects on the photocatalytic activity", *Sol. Energ. Mat. Sol. C*, **92**, 1030 (2008).
20. W. J. Li and Z. W. Fu, "Nanostructured WO_3 thin film as a new anode material for lithium-ion batteries", *Appl. Surf. Sci.*, **256**, 2447 (2010).
21. D. Chen and J. Ye, "Hierarchical WO_3 Hollow Shells: Dendrite, Sphere, Dumbbell, and Their Photocatalytic Properties", *Adv. Funct. Mater.*, **18**, 1922 (2008).
22. S. K. Deb, "Opportunities and challenges of electrochromic phenomena in transition metal oxides", *Sol. Energ. Mat. Sol. C*, **25**, 327 (1992).
23. T. Tatsuma, S. Saitoh, P. Ngaotrakanwiwat, Y. Ohko, and A. Fujishima, "Energy Storage of TiO_2-WO_3 Photocatalysis Systems in the Gas Phase", *Langmuir*, **18**, 7777 (2002).
24. P. Ngaotrakanwiwat, T. Tatsuma, S. Saitoh, Y. Ohko, and A. Fujishima, "Charge–discharge behavior of TiO_2-WO_3 photocatalysis systems with energy storage ability", *Phys. Chem. Chem. Phys.*, **5**, 3234 (2003).
25. X. H. Zhang, X. H. Lu, Y.Q. Shen, J. B. Han, L. Y. Yuan, L. Gong, Z. Xu, X. D. Bai, M. Wei, Y. X. Tong, Y. H. Gao, J. Chen, J. Zhou, and Z. L. Wang, "Three-dimensional WO_3 nanostructures on carbon paper: photoelectrochemical property and visible light driven photocatalysis", *Chem. Commun.*, **47**, 5804 (2011).
26. M. Qamar, Q. Drmosh, M. I. Ahmed, M. Qamaruddin, and Z. H. Yamani, "Enhanced Photoelectro-chemical and photocatalytic activity of WO_3-surface modified TiO_2 thin film", *Nanoscale Res. Lett.*, **10**, 54 (2015).
27. O. Arutanti, A. B. D. Nandiyanto, T. Ogi , T. O. Kim, and K. Okuyama, "Influences of Porous Structurization and Pt Addition on the Improvement of Photocatalytic Performance of WO_3 Particles", *ACS Appl. Mater. Interfaces*, **7**(5), 3009 (2015).
28. B. Palanisamy, C. M. Babu, B. Sundaravel, K. Shanthi, and V. Murugesan, "Photocatalytic Degradation of Aqueous Alachlor with Visible-Light Active Mesoporous WO_3/TiO_2 ", *Sci. Adv. Mater.*, **7**(4),746 (2015).